Microfluidic Channel Geometry and Fluid Velocity Investigation for Single Cell Hydrodynamic Trapping

Amelia Ahmad Khalili, Mohd Ariffanan Mohd Basri, Mohd Azhar Abdul Razak, Rubita Sudirman, Mohd Afzan Othman, Ismail Ariffin and Camallil Omar
Faculty of Electrical Engineering, Universiti Teknologi Malaysia, 81310 Skudai, Johor, Malaysia
ariffanan@fke.utm.my

***Abstract*—Microfluidic technology has been applied widely for separating and trapping various type of cells. This technology has open ways to study and understand the biological systems, the mechanism of diseases, developing the therapeutic drugs, strategy to cure diseases and also in developing the biomarker for early disease diagnosis. Hydrodynamic cell trapping offers a great opportunity to direct, position, and trap particles or cells in small volume liquids, a crucial requirement for efficient single cell analysis. The challenges in hydrodynamic trapping are the need for control precisely the microfluidic multiple streams and a precise geometry design required to allow successful trapping. To address this limitation, the single cell hydrodynamic trapping finite element simulation was developed to determine the efficiency of single cell traps of variable geometries. A series of simulation studies were performed to analyze the effect of the trap hole size, channel's height and fluid's flow profiles to the appropriate for efficient single cell trapping. From the simulation, increasing the trap hole size has resulted in a gradually decreased of the fluid velocity in the trap channel. Furthermore, the fluid velocity in trap channel was found increasing with the increment of the $H_{Channel}$. Single cell trapping channel with the H_{Hole} of 4 μm and $H_{Channel}$ of 15 μm produced the highest velocity in the trap channel compared to other geometry tests. This finite element model could be utilised as a guideline for designing and developing a chip to reduce the costly and time-consuming trial-and-error fabrication process.**

***Index Terms*—Cell Trapping; Hydrodynamic; Single Cell, Velocity.**

I. INTRODUCTION

Cellular studies represented by a group of cells in populations are effective in defining broad properties of cells through a variety of laboratory experimental analyses. Majority of the techniques were executed as an array of experimental treatments and cellular culture. The feedback of individual cells in response to the laboratory culture treatments are quantified as the average feedback of the collection of the individual cells. Therefore, the differences between individual cells could be deserted and this could disguise the important response of a single cell. The feedback of a collection of cells unable to screen the individual differences or alterations between cells and left out the important cellular characteristics between single cells. The infected cell might be overlooked as normal cell because the measurement representing the average of normal cells. These limitations have moved the cell-based analyses towards the studies in the single cell level.

Single cell investigation has expanded to the cell characterization, in discovering cellular properties and feedback of the single cell in response to the culture treatments as and environmental conditions. Forgoing single cell mechanical and electrical characterization were performed to study the biophysical characteristics of cells using various approaches such as Atomic Force Microscopy (AFM) [1]–[5], micropipette aspiration [6]–[8], red blood cell biomembrane probe [9]–[12] optical tweezer [13]–[15] and microfluidic channel [16]–[20]. All those techniques with the exception of the microfluidic channel necessitate the individual cell to be manually separated, extracted and manipulated manually using the micromanipulator by the experienced and skilful user. The processes to position an individual cell are often labor intensive and time consuming with the need of complicated and sophisticated instruments. Furthermore, the individual cells were analyzed in culture dishes that are open in the air, which is exposed to contamination in the environment. This condition will change the actual condition of the cells and does not mimic the conditions of cells in human body, where cells always surrounded by human body fluid in a closed and controlled condition.

A number of approaches have been employed in the microfluidic device to isolate an individual cell. For example, microwell-based [21]–[25], dielectrophoresis-based [26]–[30], and hydrodynamic-based [31]–[38] microfluidic devices have been developed for single-cell trapping due to a growing demand for high-throughput single cell manipulation with simple yet reliable tools. In microwell-based platforms, to achieve a high trapping efficiency it is required to design a precise geometry [23]. For cell trapping using dielectrophoresis technique, a non-uniform AC field is applied to manipulate polarized particles in suspension. This is a valuable approach to control a single cell efficiently. There are diverse of methods that have been developed to capture a single cell inside a microfluidic device such as techniques of microwell [21]–[25], dielectrophoresis [26]–[30], and hydrodynamic [31]–[38]. These techniques are demanding as they are proven to be reliable tools to perform a high-throughput single cell manipulation. Microwell technique requires an accurate geometry design for obtaining an efficient cell capture [23]. Dielectrophoresis is an effective technique to move the polarized cells in the fluidic environment but it could affect the cell viability and attenuate the cell proliferation. The hydrodynamic technique requires a properly designed microstructure to produce an appropriate

fluidic resistance that will drive cells to the trapping site. There are two type of hydrodynamic traps; the sieve traps [31]–[33] and small side traps [34]–[38]. The geometry of the microstructures needs to be precisely designed to enable fluids and cells in the main channel to be directed to the desired microstructures traps. Cells will be directed to the empty trap and filled the trap, and the remaining cells will by-pass the filled trap. Compared to other technique, hydrodynamic trapping is the most suitable method to capture single cells inside fluidic environment and to be integrated with other single cell characterization technique. However, the challenges in hydrodynamic trapping are the requirement of an exact control of the numerous streams, a precise channel design and geometries, optimization analysis to achieve efficient trapping and further fluid profile investigation are still required. Most of the single cell hydrodynamic traps have so far been designed by intuition and determined by trial-and-error fabrication approaches.

Reported simulations study on the hydrodynamic single cell trapping were performed using two-dimensional (2D) and three-dimensional (3D) simulation using various type of software such as CONVENTORWARE, ANSYST, and COMSOL Multiphysics [37], [39]–[41]. The study involves the analysis of fluid flow profile and fluid structure interactions. However, when it comes to the combination of fluid with solid particle simulation, the reported simulation involves the combination of the static solid particle and dynamic fluid flow. There are lacking the 3D simulation which includes the dynamic fluid-solid behavior. Improvement in implementing dynamic 3D solid structure inside fluidic environment is needed to further understand the interactions and movement of a solid structure in the fluid inside the microchannels. Furthermore, a simulation analysis that could be used as to predict the channel's trapping ability and geometry optimization is highly needed to reduce the trial-and-error fabrication processes which are costly and time-consuming.

The hydrodynamic single cell trapping capturing channel is influenced by the cell sizes and types. Divers of cells needed require unalike channel geometries and sizes. Therefore, before fabricating the real device it is crucial to investigate and optimize the channel's geometry. Furthermore, time and cost of fabrications also could be reduced. In this work, the dynamic 3D solid structure finite element simulations were created by manipulating the main channel's inlet and trap hole hydrodynamic fluid flow rate (Q). This simulation analysis presents a proof of concept of hydrodynamic single cell trapping and a guideline to design and optimize the channel geometries and fluid Q to trap a 5 µm yeast cell, *Saccharomyces cerevisiae*. The optimization of fluid Q was performed by manipulating the fluid velocities applied in the trap channel. There are three parts of the simulation study; the investigation on the effect of channel's geometry for; (a) the trap hole size (H_{Hole}) and (b) the channel's height (H_{Channel}) and lastly (c) the investigation of the fluid's flow profile in the channel that appropriate for single cell trapping.

II. Theoretical Concept

The hydrodynamic trapping theory is simplified as follows: (a) when trapping site is empty, the main channel will have a higher hydrodynamic flow resistance (*Rh)* than the trapping site; this fluidic condition will drive the cells to flow into the trapping area (Figure 1(a)-(b)); after a cell has been trapped, it will block the fluid movement into the trapping area and increase the *Rh* in the trapping area; (b) the fluidic direction will be diverted from the trapping area to the main channel, therefore next cells will be driven to bypass the occupied trapping site [42]. Figure 1 (a)-(b); depicts a graphical description of the hydrodynamic trapping concept with a yeast cell represented by the orange oval.

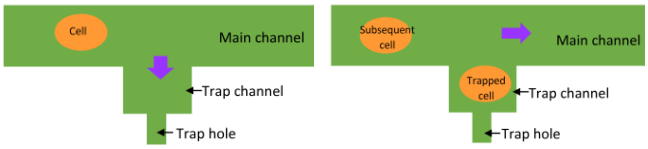

(a) (b)

Figure 1: Simple schematic of single-cell trapping channel with the hydrodynamic resistance (a) before cell trapping (b) after cell trapping.

The Darcy-Weisbach equation is utilized to determine the differences in pressure (pressure drop) within a microchannel. The flow rate (Q) is defined by Equation (1) via the Hagen–Poiseuille equation:

$$\Delta P = Q \times Rh = Q \times \left(\frac{C\mu LP^2}{A^3}\right) \tag{1}$$

where Rh, ΔP and μ represent the flow resistance, pressure drop and the fluid's viscosity of the rectangular channels, respectively. C denotes a constant which influenced by the channel's aspect ratio (ratio between height and width of the channel). The channel's length, perimeter, and cross-sectional area are symbolized by L, P, and A, respectively. From Equation (1), with the assumption that the pressure difference is same ($\Delta P_{\text{Trap}} = \Delta P_{\text{Main}}$), it can be deduced that the flow resistance ratio ($Rh_{\text{Main}}/Rh_{\text{Trap}}$) or the flow rate ratio ($Q_{\text{Trap}}/Q_{\text{Main}}$) between the trap and e main channel as Equation (2) [43]:

$$\frac{Q_{\text{Trap}}}{Q_{\text{Main}}} = \left(\frac{C_{\text{Main}}}{C_{\text{Trap}}}\right)\left(\frac{L_{\text{Main}}}{L_{\text{Trap}}}\right)\left(\frac{P_{\text{Main}}}{P_{\text{Trap}}}\right)^2\left(\frac{A_{\text{Trap}}}{A_{\text{Main}}}\right)^3 \tag{2}$$

Equation (2) can be defined from a correlation of $P = 2\,(W + H)$ and $A = W \times H$, where H and W are the height and width of the channel, respectively, as follows:

$$\frac{Q_{\text{Trap}}}{Q_{\text{Main}}} = \left(\frac{C_{\text{Main}}}{C_{\text{Trap}}}\right)\left(\frac{L_{\text{Main}}}{L_{\text{Trap}}}\right)\left(\frac{W_{\text{Main}} + H_{\text{Main}}}{W_{\text{Trap}} + H_{\text{Trap}}}\right)^2\left(\frac{W_{\text{Trap}}H_{\text{Trap}}}{W_{\text{Main}}H_{\text{Main}}}\right)^3 \tag{3}$$

Referring to Equations (2) and (3), it is known that the flow rates distribution of the trap channel (Q_{Trap}) and main channel (Q_{Main}) are dependent on the corresponding *Rh*. In order to activate the trap to function, the flow rate along the trap channel is needed to be greater than the main channel ($Q_{\text{Trap}} > Q_{\text{Main}}$). The hydrodynamic flow resistance along the main channel has to be greater than the trap channel ($Rh_{\text{Main}} > Rh_{\text{Trap}}$) to could enable a single cell trapping in the trapping site.

The hydrodynamic trapping concept for trapping sites was proposed in [35]. This concept has been widely explored and adopted for the guideline of sequential single cell entrapment

inside the microfluidic channel. However, the work is only done experimentally in order to prove the concept and no simulation works has been reported prior to the microfluidic design. This practice may be involving high costs in fabrication and consume a lot of time to get the right geometry of the devices which fabricated through trial and error. Hence, there are needs to develop a 3D finite element dynamic fluid-solid structure simulation for single cell trapping that could be used to design and determine the appropriate dimension of microfluidic channels for any kind of cells or particles prior to fabrication. There are several reported finite element simulation analyses on the hydrodynamic single cell trapping which involves the combination of fluid with solid particle; however, the simulation only involves the analysis of static solid particle and dynamic fluid flow. There is lack of the 3D simulation analysis which includes the dynamic solid behavior involving single cell hydrodynamic trapping. Improvement in implementing dynamic 3D solid structure inside fluidic environment finite element simulation is needed to further understand the interactions and movement of a solid structure in the fluid inside the microchannels.

A 3D finite element dynamic fluid-solid structure hydrodynamic single cell trapping simulation was developed to produce a finite element single cell trapping system. The variables for optimization are the geometry of the trapping channel (*L*, *H*, and *W*) and fluid flow rate (refer Equation (3)) and subject to the application, type and size that will be carried out in the channel after the cells are trapped. In this work, 3D finite element dynamic fluid-solid simulation, cells are inserted through the inlet and directed to the trap channel by varying the fluid's velocity in the trap hole (representing fluid suction in real device application). The geometry of trap channel and trap hole are varied and H_{Hole} and H_{Channel} were adapted to yield a suitable *Q* ratio which brings to successful trapping (refer Equation (3)). The subsequent cells will be forwarded via the channel's outlet by injecting cell's culture medium. Investigation study is done to find the *Q* ratio and the suitable channel's dimension to trap a 5 μm single yeast cell.

III. Simulation Setup

The analysis was carried out using a multiphysics analysis finite element software, ABAQUS-FEA™. The 3D finite element dynamic fluid-solid structure single cell hydrodynamic loop channel trapping simulation composed of the fluid channel and the sphere-shaped elastic yeast cell which modeled as a three-dimensional (3D) deformable part (Figure 2). The trap and main channel with a rectangular trap hole placed in the center, at the edge of the trap channel. The eight-node linear Eulerian brick element part assigned with water properties (viscosity, equation of state, and density) using 3D Eulerian explicit EC3DR is adopted to develop the microchannel. A 5 μm ellipse-shaped yeast cell was built as an eight-node linear brick 3D part with the yeast properties (density, Poisson's ratio, and Young's modulus) and an elastic 3D standard solid deformable C3D8R which the properties are taken from [47]–[52]. Yeast cell with 5 μm diameter was chosen in the 3D simulation as it is the average size of spherical yeast cell and the available single cell mechanical properties obtained for *Saccharomyces cerevisiae* as reported from the experimental works[47]–[52]. The simulation study was divided into three part; to investigate the effect of channel's geometry, (a) the trap hole size (H_{Hole}) and (b) the channel's height (H_{Channel}) (Figure 3(a)) and (c) to investigate the fluid flow profile in the channel for appropriate single cell trapping.

Figure 2 depicts the assembly setup. The parts were combined to perform the finite element simulation for the proposed system. A yeast cell was placed in the main channel, with a fixed the initial position (same distance between cell and trap channel) for all the simulation models. Both single cell trapping fluid channel and cell were meshed using hexahedron mesh types. The single cell trapping model consists of 5428 to 9007 mesh elements. General contact with rough tangential behavior was set as the interaction between cell and water, whereas frictionless was the interaction between the cell surface and channel's wall. The boundary condition for the channel's wall was applied with the no-inflow and non-reflecting Eulerian boundary.

To study the effects of different trap hole size (H_{Hole}), the trap hole's height is varied in the range of 3 to 12 μm (Figure 3(b)) with a fixed trap hole width (W_{Hole}) and length (L_{Hole}) of 2 μm and 5 μm, respectively. The trap channel's width (W_{Trap}), length (L_{Trap}) and height (H_{Trap}) were fixed to 7 μm, 7 μm and 15 μm, respectively with a fixed main channel's width (W_{Main}), and height (H_{Main}) of 15 μm. The effect of channel's height was investigated by varying the channel's height (representing the height of the main channel and trap channel)from 7 to 15 μm (refer Figure 3 (c)) with a fixed main channel's width (W_{Main}) of 15 μm, a fixed trap channel's width (W_{Trap}) and length (L_{Trap}) of 7 μm. Constant inlet fluid velocity of 0.1 μms^{-1} and various fluid velocity were applied at the trap hole ranging from 0.025–10.0 μms^{-1} to investigate the appropriate $Q_{\text{Trap}}/Q_{\text{Main}}$ ratio for single cell trapping. The $Q_{\text{Trap}}/Q_{\text{Main}}$ range was determined by theoretical calculation referring to Equation (1). H_{Hole} and W_{Channel} range were selected based on the range of target cell's size. Channel's height should be higher than the target cell's diameter to prevent clogging and not too high to prevent multiple cell trapping. The width of the main channel, trap channel, and trap hole (W_{Main}, W_{Channel} and W_{Hole}) were set to be 15 μm, 7 μm and 2 μm, respectively throughout the analysis. The main channel's width was set to be 15 μm due to the reported finding by Kim *et al*. [41] which stated that main channel width should be larger than the diameter to ensure the particles will receive effective drag forces to be directed into the trap channel.

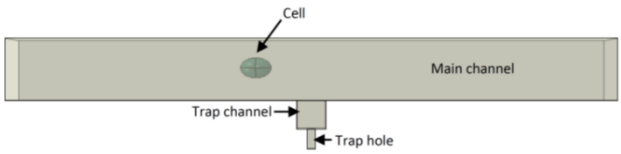

Figure 2: Construction of the 3D system and parts involved. The simulation assembly consists of eulerian part (fluid channel) and 3D deformable part (cell).

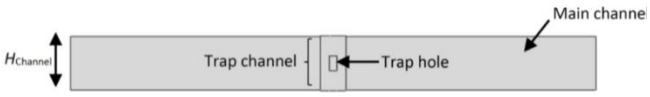

(a)

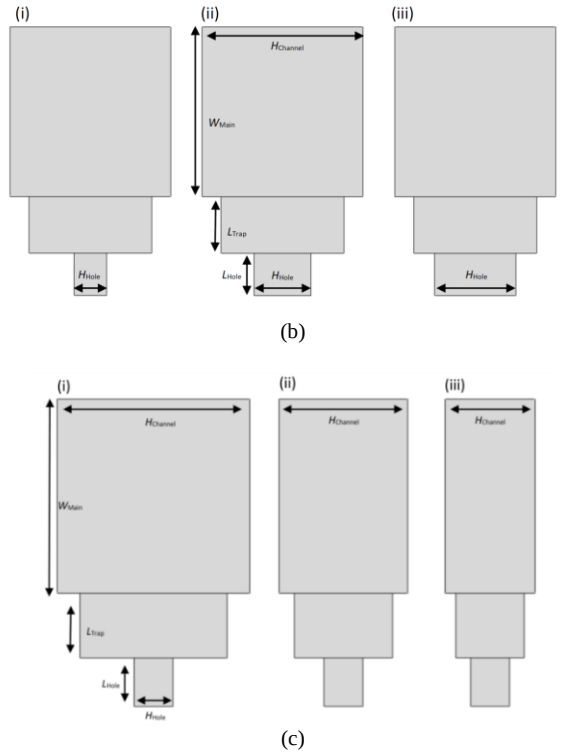

Figure 3: (a) Front view of the channels that illustrate the position of the main channel, trap channel, trap hole and channel's height ($H_{Channel}$). (b) Illustration of the single cell trapping channel from side view for different trap hole sizes (H_{Hole}) (c) Illustration of the single cell trapping channel from side view for different channel's height ($H_{Channel}$).

IV. Results and Discussion

A. Effects of Different Trap Hole Sizes

The fluid velocity profile within the trap and main channel during after and prior to cell trapping were investigated to prove the single cell hydrodynamic trapping concept. The simulation study was executed to observe the effects of different trap hole size (H_{Hole}) for the trap channel's height in the range of 3 to 12 μm. Fluid velocity applied at the trap hole was varied to comply with the desired Q_{Trap}/Q_{Main} ratio. A Single yeast cell was capable to be directed and being captured into the trapping site when Q_{Trap}/Q_{Main} ratio was 2.0 and above. Increasing the the H_{Hole} from 3 to 15 μm produced a similar trapping behavior. The yeast cell could be driven by the fluid flow and directed into the trapping site when Q_{Trap}/Q_{Main} ratio was 2.0 and above, proving that hydrodynamic single cell trapping concept works accordingly. However, different results were obtained for channels with a H_{Hole} less than 3 μm. The cell was found to bypass the trapping site and unable to be trapped although the Q_{Trap}/Q_{Main} ratio was above 2.0. This analysis shows that H_{Trap} less than 3 μm is not appropriate for the proposed channel geometry. The design was unsuccessful to obey the concept of hydrodynamic trapping, possibly because of the size of trap hole (<1/5 of H_{Trap}) is small. The small trap hole size (H_{Hole}) possibly produce low pressure drop and cause a very low fluid velocity distribution which resists cells being captured in trap channel [44]–[46]. Figure 4 shows the position of points where the velocity of fluid was measured in the main and trap channel and Figure 5 shows the graph of fluid's velocity in both main and trap channel for different Q_{Trap}/Q_{Main} ratio.

The red dashed line in Figure 5 shows the division of fluid velocity between the trap and main channel. The graphs representing the fluid velocity in the main channel were plotted above the red dashed line while the graphs representing the fluid velocity in the main channel were found to be below the line. The model of single cell trapping with the biggest size of trap hole's (H_{Hole} of 12 μm) produced the lowest fluid velocity in the trap hole while cell trapping channel with H_{Hole} of 4 μm produced the highest velocity in the trap hole for all different Q_{Trap}/Q_{Main} ratio (Figure 5). It was found that the velocity of the fluid in the trap channel increased when the trap hole size decreases with the exception of single cell trapping site with H_{Hole} of 3 μm. This probably due to the small size of the trap hole could cause a distribution of fluid velocity very low [44]–[46] and a reduction of the fluid velocity in the trap channel. However, the fluid's velocity in the main channel was found to be consistent in the range of 0.1 to 0.3 μms^{-1}. No significant increase was found in the main channel when the trap hole size was decreased. Increasing the trap hole size resulted in a gradually decreased of the fluid velocity in the trap channel. The single cell trapping channel with H_{Hole} of 4 μm was chosen for the subsequent analysis.

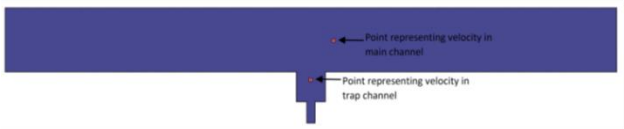

Figure 4: Two points representing the trap (left) and main (right) channel where the velocities of fluid were recorded for analysis.

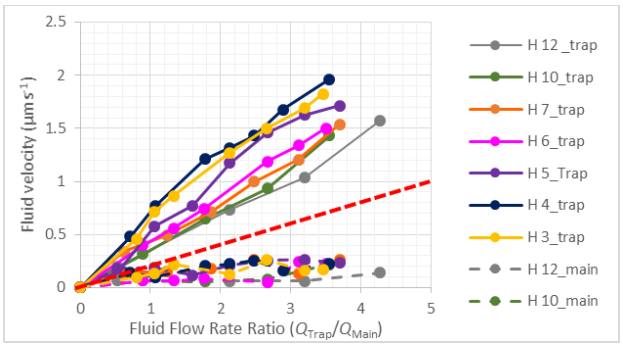

Figure 5: Graph representing the velocity of fluid inside the main and trap channel for different Q_{Trap}/Q_{Main} ratio for single cell trapping design with different trap hole size (H_{Hole}).

B. Effects of Different Channel Heights

The effectiveness of the single-cell trapping was improved by applying the appropriate trap channel's height ($H_{Channel}$), after exploring the effects of trap hole size of the single cell trapping channel. A yeast cell was used to study the effect of three different $H_{Channel}$. The manners of fluid velocities in the main and trap channel were observed for different Q_{Trap}/Q_{Main} ratio. The trap and main channel fluid's velocity during after and prior to trapping were analyzed. All the single cell trapping design with diverse $H_{Channel}$ able to isolate a single cell with Q_{Trap}/Q_{Main} ratio of 2.0 and above. The graph in Figure 6 demonstrates the result of fluid velocity inside the trap and main channel for different single cell trapping $H_{Channel}$ and Q_{Trap}/Q_{Main} ratio. In contrast with the effects of trap hole size, it was found that the fluid velocity in the trap channel increases along with the increment of the $H_{Channel}$. Single cell trapping channel with $H_{Channel}$ of 15 μm gives the highest fluid velocity in the trap channel compared to channels with a lower $H_{Channel}$ (Figure 6). Similar to the

previous analysis, no significant increase was found in the main channel when the $H_{Channel}$ was changed. The speed of the fluid in the main channel remained to be consistent in the range of 0.1 to 0.3 μms^{-1}.

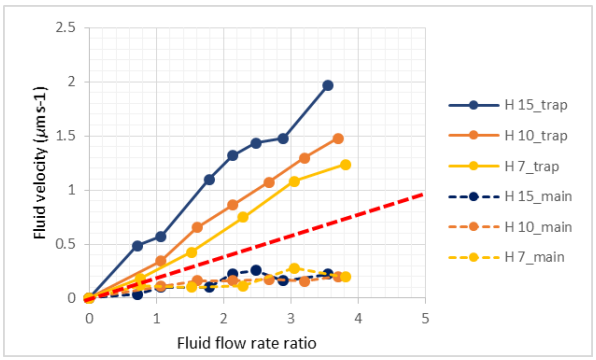

Figure 6: Graph representing the velocity of fluid inside the main and trap channel for different Q_{Trap}/Q_{Main} ratio for single cell trapping design with different channel height ($H_{Channel}$).

C. Investigation of the Fluid Flow Profile and Single Cell Trapping Channel Trapping Ability

Based on the concept of the hydrodynamic trapping proposed in [35], trapping single cell/particle can be achieved when the Q_{Trap}/Q_{Main} ratio is higher 1. The model of cell trapping with H_{Hole} and $H_{Channel}$ of 4 μm and 15 μm, respectively was used to study the appropriate Q_{Trap}/Q_{Main} ratio. The velocity of fluid applied in the inlet was varied to create a Q_{Trap}/Q_{Main} ratio range within 1 to 5. Raising the Q_{Trap}/Q_{Main} ratio was relative with the rise of the fluid's velocity applied in the trap hole. When the Q_{Trap}/Q_{Main} ratio of 2.0 or higher is selected, a yeast cell was successfully captured (Figure 7 (a)-(d)). It was found that the Q_{Trap}/Q_{Main} ratio below 2 caused the cell incapable to be trapped at the trapping site (refer Figure 7(a)). The simulation results for both the study on the effect of trap hole size and the channel height show that an Q_{Trap}/Q_{Main} ratio of 2 or higher was capable to trap a single cell and the finding was aligned with the hydrodynamic trapping concept [35].

The single cell hydrodynamic trapping mechanism was examined by investigating the fluid speed rate profile and streamline plots of the cell capturing site. Fluid velocity streamlines plots indicate the route which the fluid streams are directed, and velocity profiles describe the fluid speed rate value in the channel by color differences. Cell trapping channels with Q_{Trap}/Q_{Main} ratio below 2 (Figure 8 (a)) created velocity streamlines that were not fully concentrating on the trapping site. Fractions of the streamlines were heading to the main channel, causing the fluid streams not strong enough to drive the cell into the trapping site. This outcome was found to be aligned with the fluid's velocity dispersal formed by the same trapping channel (Figure 9 (a)). The findings demonstrate that the main channel's fluid velocity was greater than the traping site's fluid velocity for the cell trapping channel with Q_{Trap}/Q_{Main} 1. As a result, core stream will influence and drive the yeast cell to enter into the main channel's direction to bypass the trap channel.

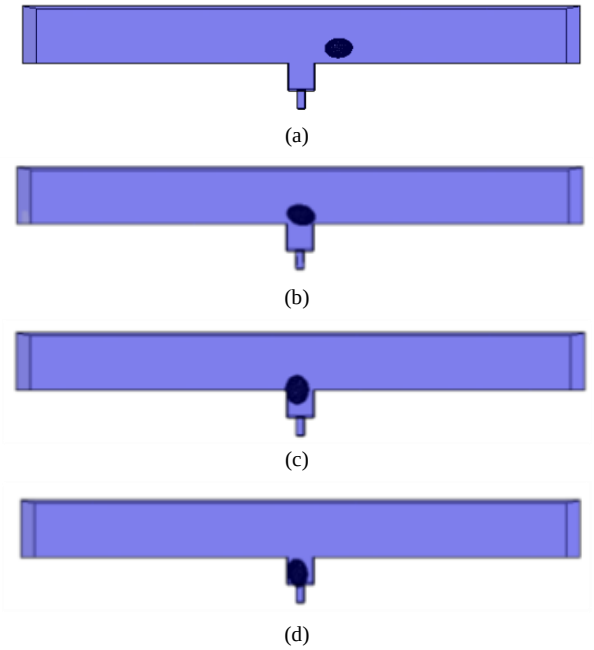

Figure 7: Single cell trapping results at simulation time of 86 s for cell trapping channel with trapping $H_{Hole}$of 4 μm and $H_{Channel}$ of 15 μm with Q_{Trap}/Q_{Main} ratio of (a) 1.0 (b) 2.0 (c) 3.0 and (d) 4.0.

The single cell hydrodynamic trapping mechanism was examined by investigating the velocity streamline field of the cell trapping site and fluid velocity profile. Velocity profiles portray the velocity value in the channel by colour differences, and fluid velocity streamlines indicate the route that where the fluid streams are heading. Cell trapping channels with Q_{Trap}/Q_{Main} ratio below 2 (Figure 8 (a)) created velocity streamlines that were not completely heading for the trapping site. Fractions of the streamlines were heading to the main channel, causing the fluid streams not strong enough to drive the cell into the trapping site. This outcome was found to be aligned with the distribution of fluid's velocity generated by the similar trapping site (Figure 9 (a)). The findings demonstrate that the main channel's fluid velocity was higher in contrast to the fluid velocity of trapping site for cell trapping channel with Q_{Trap}/Q_{Main} 1. As a result, the central stream will bring targeted particle to move into the main channel's direction to avoid the trapping site.

Different findings were obtained for cell trapping site with an Q_{Trap}/Q_{Main} ratio of 2 and higher (Figure 8 (b)-(d)), the streamlines profiles show the fluid movement deviated from the main channel to the trapping site and focused into the trapping site. The velocity distribution in the channel causes a pressure drop between the main channel and the trapping site, causing the fluid flow rate in the main channel to be lower than the trapping site. In consequence, fluid will carry cell to a lower flow resistance area to be captured. For channels with Q_{Trap}/Q_{Main} ratio of 2 to 4 (Figure 9 (b)-(d)), the distribution of fluid's velocity from the trap hole to the trapping site is larger than the main channel fluid's velocity (refer velocity value in Figure 6). These results illustrate that lower hydrodynamic resistance is produced by trapping site compared to the main channel which caused the central stream to bring the yeast-cell move to the trap channel. All channels with Q_{Trap}/Q_{Main} ratio of 2 to 4 produced same fluid velocity patterns which create sufficient pressure decrement to enable trapping in the trap channel. There was an increment of fluid velocity when the Q_{Trap}/Q_{Main} ratio was increased (refer Figure 9 (b)-(d), presented by the colour contour in

Figure 9. The cell trapping channels with a Q_{Trap}/Q_{Main} ratio of 2 and above were found capable to capture the yeast-cell with the same velocity. Nevertheless, a small variation is found in the whole time of cell trapping (total time until the cell reaches the surface of the trapping site) with diverse Q_{Trap}/Q_{Main} ratios (refer Figure 7). A Q_{Trap}/Q_{Main} ratio was found to require a less time for the complete trapping procedure in contrast to a smaller Q_{Trap}/Q_{Main} ratio.

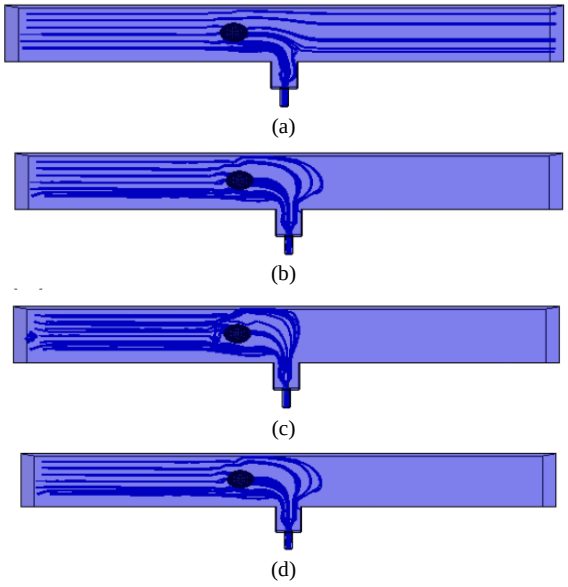

Figure 8: Velocity streamlines for cell trapping channel (top view) with H_{Hole} of 4 μm and $H_{Channel}$ of 15 μm with Q_{Trap}/Q_{Main} ratio of (a) 1.0 (b) 2.0 (c) 3.0 and (d) 4.0.

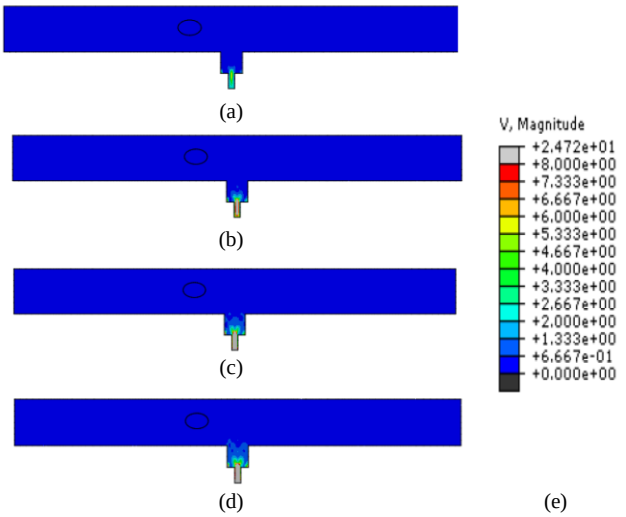

Figure 9: Fluid velocity profiles for the single cell trapping channel (top view) with H_{Hole} and $H_{Channel}$ of 4 μm and 15 μm, respectively and Q_{Trap}/Q_{Main} ratio of (a) 1.0 (b) 2.0 (c) 3.0 and (d) 4.0. (e) Fluid's velocity, V represented by the colour contours and values in μms^{-1}.

V. Conclusion

This study presents the finite element simulation of single cell trapping inside a microfluidic channel using ABAQUS-FEA™ software. The cell trapping channel shows a good agreement with the hydrodynamic resistance trapping concept. A 5 μm yeast cell model able to be a trap inside a trap channel with width and length of 7 μm by manipulating the trap hole size, channel's height and the fluid velocity in the trap hole. H_{Hole} of 4 μm and $H_{Channel}$ of 15 μm produce the highest velocity in the trap channel compared to other geometry tested. Increasing the trap hole size resulted in a gradually decreased of the fluid velocity in the trap channel and fluid velocity in trap channel increases along with the increment of the $H_{Channel}$.This cell trapping model capable to capture an individual yeast cell inside fluidic environment and could be used to study the mechanical and biological behaviour of a single cell.

Acknowledgment

This work is supported by Ministry of Higher Education (MOHE) Malaysia under the Fundamental Research Grant Scheme (FRGS) (R.J130000.7823.4F761).

References

[1] S. C. Hoffmann, A. Cohnen, T. Ludwig, and C. Watzl, "2B4 engagement mediates rapid LFA-1 and actin-dependent NK cell adhesion to tumor cells as measured by single cell force spectroscopy," *J. Immunol*., vol. 186, no. 5, pp. 2757–64, Mar. 2011.

[2] A. Beaussart, S. El-Kirat-Chatel, R.M. Sullan, D. Alsteens, P. Herman, S. Derclaye, and Y. F. Dufrêne, "Quantifying the forces guiding microbial cell adhesion using single-cell force spectroscopy," *Nat. Protoc*., vol. 9, no. 5, pp. 1049–55, May 2014.

[3] A. Engel and H. E. Gaub, "Structure and mechanics of membrane proteins," *Annu. Rev. Biochem.*, vol. 77, pp. 127–48, Jan. 2008.

[4] S.-P. Yang, C.-Y. Yang, T.-M. Lee, and T.-S. Lui, "Effects of calcium-phosphate topography on osteoblast mechanobiology determined using a cytodetacher," *Mater. Sci. Eng. C*, vol. 32, no. 2, pp. 254–262, Mar. 2012.

[5] D. J. Muller, Biochemistry, "AFM: A Nanotool in Membrane Biology," *Biochemistry*, vol. 47, pp. 7896–7898, 2008.

[6] C. P. Palmer, M. E. Mycielska, H. Burcu, K. Osman, T. Collins, R. Beckerman, R. Perrett, H. Johnson, E. Aydar, and M.B. Djamgoz, "Single cell adhesion measuring apparatus (SCAMA): application to cancer cell lines of different metastatic potential and voltage-gated Na+ channel expression," *Eur. Biophys. J.*, vol. 37, no. 4, pp. 359–68, Apr. 2008.

[7] Z. Gao, S. Wang, H. Zhu, C. Su, G. Xu, and X. Lian, "Using selected uniform cells in round shape with a micropipette to measure cell adhesion strength on silk fibroin-based materials," *Mater. Sci. Eng. C*, vol. 28, no. 8, pp. 1227–1235, Dec. 2008.

[8] R. M. Hochmuth, "Micropipette aspiration of living cells," *J. Biomech.*, vol. 33, no. 1, pp. 15–22, Jan. 2000.

[9] C. Gourier, A. Jegou, J. Husson, and F. Pincet, "A Nanospring Named Erythrocyte. The Biomembrane Force Probe," *Cell. Mol. Bioeng.*, vol. 1, no. 4, pp. 263–275, Nov. 2008.

[10] E. Evans, V. Heinrich, A. Leung, and K. Kinoshita, "Nano- to microscale dynamics of P-selectin detachment from leukocyte interfaces. I. Membrane separation from the cytoskeleton," *Biophys. J.*, vol. 88, no. 3, pp. 2288–98, Mar. 2005.

[11] E. Evans, K. Ritchie, and R. Merkel, "Sensitive Force Technique to Probe Molecular Adhesion and Structural Linkages at Biological Interfaces," vol. 68, no. June, pp. 2580–2587, 1995.

[12] E. Evans, D. Berk, and A. Leung, Biophys. "Detachment of agglutinin-bonded red blood cells. I. Forces to rupture molecular-point attachments," *Biophys. J.*, vol. 59, no. 4, pp. 838–848, Apr. 1991.

[13] M. Castelain, P. G. Rouxhet, F. Pignon, A. Magnin, and J.-M. Piau, "Single-cell adhesion probed in-situ using optical tweezers: A case study with Saccharomyces cerevisiae," *J. Appl. Phys.*, vol. 111, no. 11, p. 114701, 2012.

[14] M. Schwingel and M. Bastmeyer, "Force Mapping during the Formation and Maturation of Cell Adhesion Sites with Multiple Optical Tweezers.," *PLoS One*, vol. 8, no. 1, p. e54850, Jan. 2013.

[15] J. E. Curtis and J. P. Spatz, "Getting a Grip: Hyaluronan-Mediated Cellular Adhesion," In *Optical Science and Technology, the SPIE 49th Annual Meeting*, (International Society for Optics and Photonics, Birmingham 2004), Vol. 5514 pp. 455-466.

[16] J. Chen, Y. Zheng, Q. Tan, Y. L. Zhang, L. Yan, J. Li, W. R. Geddie, M. A. S. Jewett and Y. Sun, "A microfluidic device for simultaneous electrical and mechanical measurements on single cells," *Biomicrofluidics*, vol. 5, no. 1, p. 14113, Jan. 2011.

[17] D. Mondal, C. RoyChaudhuri, L. Das, and J. Chatterjee, "Microtrap electrode devices for single cell trapping and impedance

measurement," *Biomed. Microdevices*, vol. 14, no. 5, p. 955–964 LA–English, 2012.

[18] S. Gabriele, M. Versaevel, P. Preira, and O. Theodoly, "A simple microfluidic method to select, isolate, and manipulate single-cells in mechanical and biochemical assays," *Lab Chip*, vol. 10, no. 11, pp. 1459–1467, 2010.

[19] A. M. Forsyth, J. Wan, W. D. Ristenpart, and H. A. Stone, "The dynamic behavior of chemically 'stiffened' red blood cells in microchannel flows," *Microvasc. Res.*, vol. 80, no. 1, pp. 37–43, Jul. 2010.

[20] Y. Cho, H. S. Kim, A. Bruno Frazier, Z. G. Chen, D. M. Shin, and A. Han, "Whole-Cell Impedance Analysis for Highly and Poorly Metastatic Cancer Cells," *Microelectromechanical Systems, Journal of*, vol. 18, no. 4. pp. 808–817, 2009.

[21] G.-H. Lee, S.-H. Kim, A. Kang, S. Takayama, S.-H. Lee, and J. Y. Park, "Deformable L-shaped microwell array for trapping pairs of heterogeneous cells," *J. Micromechanics Microengineering*, vol. 25, no. 3, p. 35005, Mar. 2015.

[22] T. Sun, J. Kovac, and J. Voldman, "Image-Based Single-Cell Sorting via Dual-Photopolymerized Microwell Arrays," *Anal. Chem.*, vol. 86, no. 2, pp. 977–981, Jan. 2014.J.

[23] R. Rettig and A. Folch, "Large-Scale Single-Cell Trapping And Imaging Using Microwell Arrays," vol. 77, no. 17, pp. 5628–5634, 2005.

[24] J. Tang, R. Peng, and J. Ding, "The regulation of stem cell differentiation by cell-cell contact on micropatterned material surfaces," *Biomaterials*, vol. 31, no. 9, pp. 2470–2476, Mar. 2010.

[25] J. Doh, M. Kim, and M. F. Krummel, "Cell-laden microwells for the study of multicellularity in lymphocyte fate decisions," *Biomaterials*, vol. 31, no. 12, pp. 3422–3428, Apr. 2010.

[26] N.-C. Chen, C.-H. Chen, M.-K. Chen, L.-S. Jang, and M.-H. Wang, "Single-cell trapping and impedance measurement utilizing dielectrophoresis in a parallel-plate microfluidic device," *Sensors Actuators B Chem.*, vol. 190, pp. 570–577, Jan. 2014.

[27] M. Sen, K. Ino, J. Ramon-Azcon, H. Shiku, and T. Matsue, "Cell pairing using a dielectrophoresis-based device with interdigitated array electrodes," *Lab Chip*, vol. 13, no. 18, pp. 3650–3652, 2013.

[28] J. Voldman, M. L. Gray, M. Toner, and M. A. Schmidt, "A microfabrication-based dynamic array cytometer," *Anal. Chem.*, vol. 74, no. 16, pp. 3984–3990, Jul. 2002.

[29] R. S. Thomas, H. Morgan, and N. G. Green, "Negative DEP traps for single cell immobilisation," *Lab Chip*, vol. 9, no. 11, pp. 1534–1540, 2009.

[30] D. S. Gray, J. L. Tan, J. Voldman, and C. S. Chen, "Dielectrophoretic registration of living cells to a microelectrode array," *Biosens. Bioelectron.*, vol. 19, no. 7, pp. 771–780, Feb. 2004.

[31] I. Choi, Y. I. Yang, Y.-J. Kim, Y. Kim, J.-S. Hahn, K. Choi, and J. Yi, "Directed positioning of single cells in microwells fabricated by scanning probe lithography and wet etching methods," *Langmuir*, vol. 24, no. 6, pp. 2597–2602, 2008.

[32] A. M. Skelley, O. Kirak, H. Suh, R. Jaenisch, and J. Voldman, "Microfluidic control of cell pairing and fusion," *Nat Meth*, vol. 6, no. 2, pp. 147–152, Feb. 2009.

[33] S.-M. Kuo, C.-C. Yang, J. Shiea, and C.-H. Lin, "A post-bonding-free fabrication of integrated microfluidic devices for mass spectrometry applications," *Sensors Actuators B Chem.*, vol. 156, no. 1, pp. 156–161, Aug. 2011.

[34] W.-H. Tan and S. Takeuchi, "Dynamic microarray system with gentle retrieval mechanism for cell-encapsulating hydrogel beads," *Lab Chip*, vol. 8, no. 2, pp. 259–66, Feb. 2008.

[35] W.-H. Tan and S. Takeuchi, "A trap-and-release integrated microfluidic system for dynamic microarray applications.," *Proc. Natl. Acad. Sci. U. S. A.*, vol. 104, no. 4, pp. 1146–1151, Jan. 2007.

[36] L. M. Lee and A. P. Liu, "A microfluidic pipette array for mechanophenotyping of cancer cells and mechanical gating of mechanosensitive channels," *Lab Chip*, vol. 15, no. 1, pp. 264–273, 2015.

[37] L. M. Lee, and A. P. Liu, "A microfluidic pipette array for mechanophenotyping of cancer cells and mechanical gating of mechanosensitive channels," *Lab Chip*, vol. 15, no. 1, pp. 264–273, 2015.

[38] M. Kim, J.-W. Ahn, U.-H. Jin, D. Choi, K.-H. Paek, and H.-S. Pai, "Activation of the programmed cell death pathway by inhibition of proteasome function in plants," *J. Biol. Chem.*, vol. 278, no. 21, pp. 19406–15, May 2003.

[39] R. D. Sochol, M. E. Dueck, S. Li, L. P. Lee, and L. Lin, "Hydrodynamic resettability for a microfluidic particulate-based arraying system.," *Lab Chip*, vol. 12, no. 23, pp. 5051–6, Dec. 2012.

[40] T. Arakawa, M. Noguchi, K. Sumitomo, Y. Yamaguchi, and S. Shoji, "High-throughput single-cell manipulation system for a large number of target cells," *Biomicrofluidics*, vol. 5, no. 1, p. 14114, Jan. 2011.

[41] J. Kim, J. Erath, A. Rodriguez, and C. Yang, "A high-efficiency microfluidic device for size-selective trapping and sorting," *Lab Chip*, vol. 14, no. 14, pp. 2480–2490, 2014.

[42] T. Teshima, H. Ishihara, K. Iwai, A. Adachi, and S. Takeuchi, "A dynamic microarray device for paired bead-based analysis," *Lab Chip*, vol. 10, no. 18, pp. 2443–8, Sep. 2010.

[43] I. Kumano, K. Hosoda, H. Suzuki, K. Hirata, and T. Yomo, "Hydrodynamic trapping of Tetrahymena thermophila for the long-term monitoring of cell behaviors," *Lab Chip*, vol. 12, no. 18, pp. 3451–3457, Sep. 2012.

[44] A. Ahmad Khalili, M. R. Ahmad, M. Takeuchi, M. Nakajima, Y. Hasegawa, and R. Mohamed Zulkifli, "Hydrodynamic trapping of Tetrahymena thermophila for the long-term monitoring of cell behaviors.," *Lab Chip*, vol. 12, no. 18, pp. 3451–3457, Sep. 2012.

[45] A. A. Khalili and M. R. Ahmad, "Numerical Analysis of Hydrodynamic Flow in Microfluidic Biochip for Single-Cell Trapping Application.," *Int. J. Mol. Sci.*, vol. 16, no. 11, pp. 26770–85, 2015.

[46] A. A. Khalili, M. A. M. Basri, and M. R. Ahmad, "Simulation of Single Cell Trapping via Hydrodynamic Manipulation," *J. Teknol.*, vol. 69, no. 8, pp. 121–126, 2014.

[47] T. Gervais, J. El-Ali, A. Günther, and K. F. Jensen, "Flow-induced deformation of shallow microfluidic channels," *Lab Chip*, vol. 6, no. 4, pp. 500–7, Apr. 2006.

[48] A. K. Bryan, A. Goranov, A. Amon, and S. R. Manalis, "Measurement of mass, density, and volume during the cell cycle of yeast," *Proc. Natl. Acad. Sci. U. S. A.*, vol. 107, no. 3, pp. 999–1004, Jan. 2010.

[49] A. E. Smith, Z. Zhang, C. R. Thomas, K. E. Moxham, and A. P. Middelberg, "The Mechanical Properties of Saccharomyces Cerevisiae," *Proc. Natl. Acad. Sci. U. S. A.*, vol. 97, no. 18, pp. 9871–4, Aug. 2000.

[50] J. D. Stenson, C. R. Thomas, and P. Hartley, "Modelling the mechanical properties of yeast cells," *Chem. Eng. Sci.*, vol. 64, no. 8, pp. 1892–1903, Apr. 2009.

[51] J. D. Stenson, P. Hartley, C. Wang, and C. R. Thomas, "Determining the mechanical properties of yeast cell walls," *Biotechnol. Prog.*, vol. 27, no. 2, pp. 505–12, 2011.

[52] T. P. Burg, M. Godin, S. M. Knudsen, W. Shen, G. Carlson, and J. S. Foster, "Weighing of biomolecules, single cells and single nanoparticles in fluid.," *Nature*, vol. 446, no. 7139, pp. 1066–9, May 2007.